Ordered Mesoporous Silicoboron Carbonitride Materials via Preceramic Polymer Nanocasting

Xing-Bin Yan,* Laura Gottardo, Samuel Bernard, Philippe Dibandjo, Arnaud Brioude, Hicham Moutaabbid, and Philippe Miele*

Laboratoire des Multimateriaux et Interfaces (UMR CNRS 5615), Université Lyon 1, Université de Lyon, 43 boulevarde du 11 Novembre 1918, 69622 Villeurbanne Cedex, France

Received October 31, 2007. Revised Manuscript Received May 9, 2008

Highly ordered two-dimensional (2D) mesoporous silicoboron carbonitride (SiBCN) materials were prepared by a double nanocasting approach using mesoporous SBA-15 silica as starting template. The latter was converted into its negative replica CMK-3 carbon template, which was subsequently impregnated with a boron-modified polysilazanes of the type $[B(C_2H_4SiCH_3NCH_3)_3]_n$ ($[C_{14.4}H_{31.4}N_{4.1}B_{1.0}Si_{3.0}]_n$) using a liquid-phase impregnation (LPI) process. The derived $[B(C_2H_4SiCH_3NCH_3)_3]_n$-carbon composite was cross-linked under ammonia at 200 °C and then thermolyzed under nitrogen at 1000 °C to generate a SiBCN-carbon composite. The carbon template was subsequently removed through thermal treatment at 1000 °C in an ammonia atmosphere to generate ordered mesoporous structures. XRD and TEM analyses revealed that as a negative replica of the CMK-3 template, the obtained amorphous mesoporous material exhibited open, continuous, and ordered 2D hexagonal frameworks, whereas elemental analyses indicated the formation of materials with an empirical formula of $Si_{3.0}B_{1.0}C_{4.2}N_{3.5}$. The ordered mesoporous $Si_{3.0}B_{1.0}C_{4.2}N_{3.5}$ material displayed high surface area (600 $m^2\ g^{-1}$), high pore volume (0.61 $cm^3\ g^{-1}$), and narrow pore size distribution (around 3.4 nm) and exhibited a relatively good thermal stability in air through heat-treatment to 1400 °C.

1. Introduction

Nonoxide silicon-based ceramics derived from preceramic polymers, such as polycarbosilane-derived silicon carbide (SiC) and polysilazane-derived silicon nitride (Si_3N_4) have been investigated intensively in various research areas due to their excellent mechanical and functional characteristics.[1–3] In addition to these stable binary phases, polymer-derived multinary nitride ceramics such as SiCN, SiAlCN, SiBCN and SiBAlCN that are processed by thermolysis of modified polycarbosilazanes has emerged as a new type of thermostructural Si-based materials in the past decade.[4–14] Compared to conventional Si-based ceramics, the high-temperature properties of such metastable structures, i.e., thermal stability against crystallization and phase separation, oxidation resistance, mechanical strength, and creep resistance, have been proven to be drastically enhanced. In particular, the SiBCN composition displays a set of properties which have attracted considerable interest for the formation of materials dedicated to thermo-structural applications including fibers and matrices[6,8,10] The polymer-derived ceramics (PDCs) approach plays a major role in the performance and application of such materials. The control of the polymer composition at atomic scale, the ability to prepare near net-shaped materials, and the possibility to design the nanostructure offer ceramic properties that are difficult to find in materials produced by conventional approach such as the comelting of different nitrides.

Because of the high durability of SiBCN ceramics, which was confirmed in the course of investigations published in refs 5, 6, 8, and 10, it is reasonable to suggest that polymer-derived SiBCN materials can be regarded as a promising effective catalyst support in devices that have to withstand harsh oxidative and thermal environments. However, the complex-shaped SiBCN materials which are reported in the

* Corresponding author. E-mail: Xing-Bin.Yan@univ-lyon1.fr (X.-B.Y.); miele@univ-lyon1.fr (P.M.). Fax: 33 (0) 4-72-44-06-18. Tel: 33 (0) 4-72-43-10-29.

(1) Riedel, R.; Passing, G.; Schonfelder, H.; Brook, R. J. *Nature* **1992**, *355*, 714.
(2) Kroke, E.; Li, Y. L.; Konetschny, C.; Lecomte, E.; Fasel, C.; Riedel, R. *Mater. Sci. Eng., R* **2000**, *26*, 97.
(3) Riedel, R.; Mera, G.; Hauser, R.; Klonczynski, A. *J. Ceram. Soc. Jpn.* **2006**, *114*, 425.
(4) Bill, J.; Aldinger, F. *Adv. Mater.* **1995**, *7*, 775.
(5) Riedel, R.; Kienzle, A.; Dressler, W.; Ruwisch, L.; Bill, J.; Aldinger, F. *Nature* **1996**, *382*, 796.
(6) Baldus, P.; Jansen, M.; Sporn, D. *Science* **1999**, *285*, 699.
(7) Gregory, G.; Kleebe, H.-J.; Brequel, H.; Enzo, S.; Ziegler, G. *J. Non-Cryst. Solids* **2005**, *351*, 1393.
(8) (a) Bernard, S.; Weinmann, M.; Gerstel, P.; Miele, P.; Aldinger, F. *J. Mater. Chem.* **2005**, *15*, 289. (b) Bernard, S.; Weinmann, M.; Cornu, D.; Miele, P.; Aldinger, F. *J. Eur. Ceram. Soc.* **2005**, *25*, 251.
(9) Berger, F.; Weinmann, M.; Aldinger, F.; Müller, K. *Chem. Mater.* **2004**, *16*, 919.
(10) (a) Weinmann, M.; Schuhmacher, J.; Kummer, H.; Prinz, S.; Peng, J. Q.; Seifert, H. J.; Christ, M.; Muller, K.; Bill, J.; Aldinger, F. *Chem. Mater.* **2000**, *12*, 623. (b) Weinmann, M.; Kamphowe, T. W.; Schuhmacher, J.; Müller, K.; Aldinger, F. *Chem. Mater.* **2000**, *12*, 2112.
(11) Weinmann, M.; Kroschel, M.; Jäschke, T.; Nuss, J.; Jansen, M.; Kolios, G.; Morillo, A.; Tellaeche, C.; Nieken, U. *J. Mater. Chem.* **2008**, *18*, 1810.
(12) (a) Haberecht, J.; Krumeich, F.; Grützmacher, H.; Nesper, R. *Chem. Mater.* **2004**, *16*, 418. (b) Haberecht, J.; Nesper, R.; Grützmacher, H. *Chem. Mater.* **2005**, *17*, 2340.
(13) Müller, A.; Gerstel, P.; Butchereit, E.; Nickel, K. G.; Aldinger, F. *J. Eur. Ceram. Soc.* **2004**, *24*, 3409.
(14) Nghiem, Q.-D.; Kim, D.-P. *J. Mater. Chem.* **2005**, *15*, 2188.

10.1021/cm703114y CCC: $40.75
Published on Web 09/30/2008

literature including fibers,[6,8] composites,[10b] and films[14] have a low specific surface area and therefore are not suitable for catalytic applications. As a consequence, the demand for high surface area and uniform porosity in such applications makes the preparation of mesoporous SiBCN ceramics an attractive challenge.

Nanocasting represents a method for creating organized and mesostructured materials based on replicating nanoscale structures via a direct-templating process (hard template). Mesoporous carbon,[15–17] oxides,[18,19] sulfides,[20] and metal[21] as well as mesoporous metal oxides[22] and silica[23] have been prepared by using mesostructured silica and carbon as templates. There are few reports dedicated to periodic ordered mesoporous ceramics derived from preceramic polymers.[24–35] Recently, we have succeeded in the preparation of mesoporous boron nitride materials using hard templates.[24] Concerning Si-based mesoporous materials, SiC[26–29] and SiCN[30–35] materials have also been prepared using the casting approach, but to date, no report has shown that multielemental porous SiBCN materials could be synthesized using the conbination between a nanocasting pathway and the PDCs approach. This is probably caused by the lack of a preceramic polymer, which is especially designed for the nanocasting through a liquid-phase impregnation (LPI) process.

In this contribution, we demonstrate the successful synthesis of ordered 2D hexagonal mesoporous SiBCN materials with high Brunauer−Emmett−Teller (BET) surface area and uniform pore size by nanocasting mesoporous carbon template (CMK-3) with a preceramic polymer of the type $[B(C_2H_4SiCH_3NCH_3)_3]_n$.

2. Experimental Section

2.1. General Comments. All synthesis reactions involving the synthesis and nanocasting of the SiBCN polymer were carried out in a purified argon atmosphere passing through successive columns of BTS-catalyst and potassium hydroxide by means of standard Schlenk manipulations and vacuum/argon-line techniques. Manipulation of the polymer, mesoporous, and bulk samples were made inside an argon-filled glovebox (Jacomex BS521). Triblock poly(ethylene oxide)-*b*-poly(propylene oxide)-*b*-poly(ethylene oxide) copolymer Pluronic P123 (M_w = 5800, $EO_{20}PO_{70}EO_{20}$) was purchased from Sigma-Aldrich. Dichloromethylvinylsilane $CH_2{=}CHSiCH_3Cl_2$ was obtained from Sigma-Aldrich and freshly distilled from magnesium at 115 °C at P_{atm} before use. Borane dimethylsulfide $BH_3{\cdot}S(CH_3)_2$ (2 M solution in toluene) was obtained from Sigma-Aldrich and used as-received. Methylamine anhydrous (Sigma-Aldrich, 99+%) was used in its as-received state as a linking reagent during the polymerization process. Tetrahydrofuran (THF) and toluene were purified by distillation from sodium using benzophenone. Nitrogen and ammonia with electronic quality (Air liquide) were used in their as-received state during the ceramic preparation. Millipore water was used in the syntheses of silica and carbon templates.

2.2. Synthesis of the Boron-Modified Polysilazane $[B(C_2H_4SiCH_3NCH_3)_3]_n$. The boron-modified polysilazane was obtained according to a monomer route by hydroboration of a dichloromethylvinylsilane, followed by aminolysis of the tris(dichloromethylsilylethyl)borane derived therefrom and following standard procedures.[5,10a]

The synthesis of the tris(dichloromethylsilylethyl)borane, $B(C_2H_4SiCH_3Cl_2)_3$ (C_2H_4 = $CHCH_3$, CH_2CH_2), was performed from $CH_2{=}CHSiCH_3Cl_2$ according to procedures described in the literature.[5,36,37] The residual oil was purified by vacuum distillation (1×10^{-2} mbar/117 °C) via an ether bridge to deliver a colorless oil.

The synthesis of the boron-modified polysilazane, $[B(C_2H_4SiCH_3NCH_3)_3]_n$ (C_2H_4 = $CHCH_3$, CH_2CH_2), was performed from the tris(dichloromethylsilylethyl)borane, $B(C_2H_4SiCH_3Cl_2)_3$ (C_2H_4 = $CHCH_3$, CH_2CH_2) in THF at 0 °C by passing methylamine through the solution under vigorous stirring according to our previously reported paper.[8] When the reaction has ended, the temperature was allowed to warm up to RT then kept at this temperature under vigorous stirring overnight. Filtration of the methylamine hydrochloride from the reaction mixture and distillation of the solvent led to a colorless soluble powder that is very sensitive to moisture and air. Anal. Found (wt %): C, 47.7; H, 8.7; N, 15.7; B, 3.0; Si, 23.2; O, 0.4. $[C_{12}H_{30}N_3BSi_3]_n$ ([311.46]$_n$) Calcd: C, 46.25; H, 9.70; N, 13.54; B, 3.42; Si, 27.04. IR (KBr/cm^{-1}): ν (N−H) = 3425, 3321, 3229 *w*; ν (C−H) = 2954 *s*, 2898 *s*, 2803 *m*; $\delta_{asym}(CH_3)$ = 1463 *w*; ν(C−C) = 1355 *w*; δ(Si-CH_3) = 1260 *s*; δ(C−B−C) = 1187 *m*; δ(SiCH_2C) = 1139 *m*;ν(C−N) = 1061 *m*; δ (N−Si−N) = 914 *sh*-875 vs. Chemical shift values in NMR spectra are reported in parts per million relative to $(CH_3)_4Si$ (^{1}H, ^{13}C; δ = 0). ^{1}H NMR ($CDCl_3$): δ 0.32 (br, SiCH_3), 0.66 (vbr, SiCH_2CH$_2$B), 0.98 (br, CH_3CHBSi), 1.01 (br, SiCH$_2$CH_2B), 1.30 (br, CH$_3$C*H*BSi), 2.77 (vbr, N−CH_3). ^{13}C NMR ($CDCl_3$): δ 4.09 (Si*C*H$_3$), δ 10.87 (Si*C*H$_2$CH$_2$B), δ 26.26 (CH$_3$*C*HBSi), 29.62 (NH*C*H$_3$), 30.48 (*C*H$_3$CHBSi), 31.74 (N*C*H$_3$). TGA (NH_3 (200 °C) + N_2 (1000 °C), 48.7% ceramic yield): 25−200 °C, Δm = 19.3%; 200−1000 °C, Δm = 32%.

(15) Ryoo, R.; Joo, S. H.; Jun, S. *J. Phys. Chem.* **1999**, *103*, 7743.
(16) Jun, S.; Joo, S. H.; Ryoo, R.; Kruk, M.; Jaroniec, M.; Liu, Z.; Ohsuma, T.; Terasaki, O. *J. Am. Chem. Soc.* **2000**, *122*, 10712.
(17) Lee, J.; Han, S.; Hyeon, T. *J. Mater. Chem.* **2004**, *14*, 478.
(18) Jiao, K.; Zhang, B.; Yue, B.; Ren, Y.; Liu, S.; Yan, S.; Dickinson, C.; Zhou, W.; He, H. *Chem. Commun.* **2005**, 5618.
(19) Tian, B.; Liu, X.; Solovyov, L. A.; Liu, Z.; Yang, H. *J. Am. Chem. Soc.* **2004**, *126*, 865.
(20) Gao, F.; Lu, Q.; Zhao, D. *Adv. Mater.* **2003**, *15*, 739.
(21) Shin, H. J.; Ryoo, R.; Liu, Z.; Terasaki, O. *J. Am. Chem. Soc.* **2001**, *123*, 1246.
(22) Dong, A.; Ren, N.; Tang, Y.; Wang, Y.; Zhang, Y.; Hua, W.; Gao, Z. *J. Am. Chem. Soc.* **2003**, *125*, 4976.
(23) Kang, M.; Yi, S. H.; Lee, H. I.; Yie, J. E.; Kim, J. M. *Chem. Commun.* **2002**, 1944.
(24) Dibandjo, P.; Bois, L.; Chassagneux, F.; Cornu, D.; Letoffe, J. M.; Toury, B.; Babonneau, F.; Miele, P. *Adv. Mater.* **2005**, *17*, 571.
(25) Vinu, A.; Terrones, M.; Golberg, D.; Hishita, S.; Ariga, K.; Mori, T. *Chem. Mater.* **2005**, *17*, 5887.
(26) Shi, Y. F.; Meng, Y.; Chen, D. H.; Cheng, S. J.; Chen, P.; Yang, H. F.; Wan, Y.; Zhao, D. Y. *Adv. Funct. Mater.* **2006**, *16*, 561.
(27) Krawiec, P.; Geiger, D.; Kaskel, S. *Chem. Commun.* **2006**, 2469.
(28) Yan, J.; Wang, A. J.; Kim, D. P. *J. Phys. Chem. B* **2006**, *110*, 5429.
(29) Sonnenburg, K.; Adelhelm, P.; Antonietti, M.; Smarsly, B.; Nöske, R.; Strauch, P. *Phys. Chem. Chem. Phys.* **2006**, *8*, 3561.
(30) Yan, J.; Wang, A. J.; Kim, D. P. *Microporous Mesoporous Mater.* **2007**, *100*, 128.
(31) Shi, Y. F.; Wan, Y.; Zhai, Y. P.; Liu, R. L.; Meng, Y.; Tu, B.; H, F.; Zhao, D. Y. *Chem. Mater.* **2007**, *19*, 1761.
(32) Yang, H.; Deschatelets, P.; Brittain, S. T.; Whitesides, G. M. *Adv. Mater.* **2001**, *13*, 54.
(33) Kamperman, M.; Garcia, C. B. W.; Du, P.; Ow, H.; Wiesner, U. *J. Am. Chem. Soc.* **2004**, *126*, 14708.
(34) Garcia, C. B. W.; Lovell, C.; Curry, C.; Faught, M.; Zhang, Y. M.; Wiesner, U. *J. Polymer Sci. B: Polymer Phys.* **2003**, *41*, 3346.
(35) Nghiem, Q. D.; Kim, D. P. *Adv. Mater.* **2007**, *19*, 2351.
(36) Weinmann, M.; Haug, R.; Aldinger, F.; Schuhmacher, J.; Müller, K. *J. Organomet. Chem.* **1997**, *541*, 345.
(37) Kienzle, A. Thesis. Universität Stuttgart, Stuttgart, Germany, 1994 (in German).

2.3. Synthesis of Mesoporous Silica SBA-15. Mesoporous silica SBA-15 hard template was prepared by hydrothermal synthesis according to established procedures.[38] In a typical experiment, 16.0 g of triblock copolymer P123 were dissolved in a solution of 480 g of 2 M HCl and 60 g of water under stirring at 35 °C for 6 h. Thirty-four grams of TEOS (tetraethyl orthosilicate) was then added under vigorous stirring, and the mixture was kept at 35 °C for 20 h. The solution was next heated to 90 °C for 3 days. The white solid was recovered by filtration, washed with deionized water, and dried. The product was then calcined in air at a heating rate of 1 °C min^{-1} up to 500 °C and kept 6 h at this temperature. The homemade SBA-15 template displayed the two-dimensional *P6mm* hexagonal symmetry with specific surface area of 851 m^2 g^{-1} and pore diameters of 7.9 nm.

2.4. Synthesis of Mesoporous Carbon CMK-3. Mesoporous carbon CMK-3 was synthesized by the nanocasting pathway using sucrose as a precursor and mesoporous silica SBA-15 as a hard template according to the literature.[15] In a typical experiment, 5.0 g of SBA-15 were placed in a Schlenk-type flask, dehydrated at 150 °C under a vacuum for 4 h and cooled down to RT. For the preparation of the carbon, 6.25 g of sucrose were added to a mixture of 25 g of H_2O and 0.70 g of H_2SO_4 (95−97 wt %) under stirring. After complete dissolution of the sucrose, the SBA-15 was added to the solution and then mixed under vigorous stirring for a first LPI process. The resulting viscous mixture was stirred for 2 days and subsequently heated in an oven at 100 and 160 °C for 6 h, respectively. A second LPI process was made. The resulting powder was mixed with a sucrose solution consisting of 4.0 g of sucrose, 25 g of H_2O, and 0.45 g of H_2SO_4 (95−97 wt %). After being treated at 100 and 160 °C for 6 h as applied during the first attempt, carbonization was carried out in a graphite furnace under a vacuum at 900 °C (60 °C h^{-1}) and kept 3 h at this temperature. The resulting silica−carbon composite was washed by stirring in 1 M NaOH solution (50 vol % water and 50 vol % ethanol) at 100 °C in two times. After being washed with ethanol and dried at 120 °C, 2.3 g of CMK-3 were collected as black powders. The CMK-3 template exhibited a highly ordered 2D hexagonal mesostructure with a specific surface area of 1035 cm^2 g^{-1} and pore diamters of 3.2 nm.

2.5. Preparation of Mesoporous SiBCN Materials. Nanocasting of the boron-modified polysilazanes of the type $[B(C_2H_4SiCH_3NCH_3)_3]_n$ was carried out through a LPI process in a Schlenk-type flask similar to that used in our previous reports for preparing mesoporous boron nitride.[24] Six-tenths of a gram of $[B(C_2H_4SiCH_3NCH_3)_3]_n$ was dissolved in 1.5 mL of THF under stirring. Before being impregnated, 0.5 g of CMK-3 template were dehydrated at 100 °C for 2 h under a vacuum (1×10^{-2} mbar), and then cooled to RT. The CMK-3 was added in an argon atmosphere to the polymer solution under stirring at RT and kept for 24 h at this temperature. After absorption of the polymer into the channels of the template, the solvent was evaporated in a high vacuum (RT/1×10^{-2} mbar) to generate a black powder. The Schlenk-type glass containing the polymer was equipped with a gas inlet tube to introduce a stream of ammonia (40 mL min^{-1}) and was subsequently heated uniformly to 200 °C under ammonia in an oil bath and held at this temperature for 2 h to cross-link the polymer and transform it into an infusible material. When the reaction has ended, it is necessary to purge with argon to eliminate ammonia during cooling to RT under constant flow (50 mL min^{-1}). A second impregnation cycle was required for completely wetting the CMK-3 template. The as-received composite was reimpregnated with a solution consisting of 0.4 g of $[B(C_2H_4SiCH_3NCH_3)_3]_n$ and 1.5 mL of THF. After being dried and cross-linked as described above, the cross-linked $[B(C_2H_4SiCH_3NCH_3)_3]_n$−carbon composite was introduced into a glovebox under nitrogen, put in an alumina crucible, and then transferred into a silica tube inserted in a horizontal tube furnace (Gero Model type F-A 150−500/13) and connected to the glovebox. The tube was pumped under a vacuum for 2 h and refilled with nitrogen (99.995%). Subsequently, samples were subjected to a cycle of ramping of 1 °C min^{-1} to 1000 °C, dwelling there for 2 h, and then cooling to RT at 5 °C min^{-1}. A constant flow (120 mL min^{-1}) of nitrogen was passed through the tube. After this polymer-to-ceramic conversion process, the composite underwent a final thermal treatment in an ammonia flow (120 mL min^{-1}) from RT to 1000 °C and kept at this temperature for 5 h to remove the carbon CMK-3 template and generate the SiBCN mesoporous material. TGA of the SiBCN−carbon composite (NH_3, 1000 °C, 48.9% weight loss): 25−720 °C, $\Delta-=0\%$; 720−1000 °C, $\Delta m = 48.9\%$. TGA of the SiBCN material (NH_3, 1000 °C, 1.2% weight loss): 25−250 °C: $\Delta m = 0\%$; 250−1000 °C: $\Delta m = 1.2\%$.

A bulk SiBCN material was prepared with the aim of investigate and then comparing the chemical composition and structural arrangement with those of the mesoporous material. The bulk SiBCN material was prepared under the same thermal conditions (cross-linking from RT to 200 °C under ammonia in an oil bath, then thermolysis under nitrogen from 200 to 1000 °C at the heating rate of 1 °C min^{-1} with a dwelling time of 2 h in a silica furnace) from the same polymer. The latter was previously crushed then sieved (<32 μm) inside the glovebox. The derived powders were put in an alumina crucible to undergo the cross-linking and thermolysis processes.

2.6. Characterization. Chemical analyses of the polymer, the mesoporous material and the bulk material were made at the Service Central de Microanalyse du CNRS (Vernaison, France). ^1H and ^{13}C NMR spectra were obtained for the polymer using a Bruker AM300 spectrometer in $CDCl_3$ operating at 300 and 62.5 MHz, respectively. Fourier transform infrared data (FT-IR) of the polymer were recorded from KBr pellets containing the polymer (Model Nicolet Magna 550 Fourier transform-infrared spectrometer). Thermogravimetric analysis (TGA) of the polymer-to-ceramic conversion was recorded on a Setaram TGA 92 16.18. Experiments were performed at 0.5 °C min^{-1} from 25 to 200 °C under ammonia, kept at this temperature for 2 h, then from 200 to 1000 at 1 °C min^{-1} under nitrogen using silica crucibles (sample weight of ∼40 mg) at ambient atmospheric pressure. TGA of the SiBCN-carbon composite and the SiBCN material were made at 1 °C min^{-1} under ammonia from RT to 1000 °C. Low-angle powder X-ray diffraction (LA-XRD) patterns were achieved using a Philipps PW 3040/60 X'Pert PRO X-ray diffraction system operating at 30 mA and 40 kV, and the patterns were acquired between 0.5° and 6° with a step size of 0.0167°. In addition, X-ray diffraction was applied from 20 to 80° to identify the global structure of the material. Infrared spectroscopy of the mesoporous and bulk SiBCN materials were taken with a Nicolet 380 FT-IR spectrometer coupled with the Attenuated Total Reflectance (ATR) accessory. A Renishaw model RM 1000 Raman microscope operating at $\lambda = 514.5$ nm was used for Raman spectroscopy.

The morphology of the initial hard templates and the final product was observed on a scanning electron microscope (SEM, Hitachi S800) operating at 15 kV. The TEM images were taken with a TOPCON EM002B transmission electron microscope operated at 200 kV. All samples were first dispersed in ethanol and then collected using carbon-film-covered copper grids for analysis. The XPS measurement of the final product was performed on a Perkin-Elmer PHI-5702 multifunctional X-ray photoelectron spectroscope

(38) Zhao, D. Y.; Feng, J. L.; Huo, Q. S.; Melosh, N.; Fredrickson, G. H.; Chmelka, B. F.; Stucky, G. D. *Science* **1998**, *279*, 548.

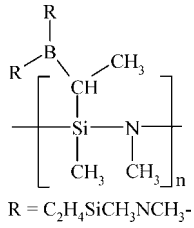

Figure 1. Basic structural units of the boron-modified polysilazane of the type $[B(C_2H_4SiCH_3NCH_3)_3]_n$ (C_2H_4 = $CHCH_3$, CH_2CH_2).[8] It should be mentioned that the boron atom may be linked to either the α- or β-position of the vinyl unit caused by the lack of regioselectivity of the dimethylsulfide borane used during hydroboration.[39]

(Physical Electronics, USA), using Al Kα radiation (photon energy 1476.6 eV) as the excitation source and the binding energy of Au (Au $4f_{7/2}$: 84.00 eV) as the reference. Nitrogen adsorption/desorption isotherms were measured on a Sorptomatic1900 analyzer (Fisons). Before adsorption measurements, the samples were outgassed for 4 h at 150 °C in the degas port of the adsorption analyzer. The Brunauer−Emmett−Teller (BET) method was used to calculate the specific surface areas. The pore size distributions were derived from the adsorption branches of the isotherms using the Barrett−Joyner−Halenda (BJH) method. The total pore volumes, V_p, were estimated from the amount adsorbed at a relative pressure of $P/P_0 = 0.99$. High-temperature thermogravimetric analysis (HT-TGA, Mettler Toledo TGA/SDTA 851 equipment) of mesoporous SiBCN materials was performed in air from 25 to 1400 °C at a heating rate of 10 °C min^{-1} using platinum crucibles.

3. Results and Discussion

3.1. Polymer Synthesis. The polymer synthesis is based on the general two-step monomeric concept which was developped by Riedel et al.,[5] then Weinmann et al.[10a] to prepare boron-modified polysilazanes of the type $[B(C_2H_4SiRNH)_3]_n$ (C_2H_4 = $CHCH_3$, CH_2CH_2; R = CH_3,[5,10a] H[10a]) in toluene using borane dimethylsulfide as hydroboration reagent and ammonia as linking agent. According to this concept, we prepared a boron-modified polysilazane of the type $[B(C_2H_4SiCH_3NCH_3)_3]_n$ (C_2H_4 = $CHCH_3$, CH_2CH_2) that can be described by the structural units given in Figure 1.[8]

This polymer ($[C_{14.4}H_{31.4}N_{4.1}B_{1.0}Si_3]_n$; oxygen values were found to be lower than 2 wt% and were therefore omitted) was obtained by the quantitative hydroboration of the vinyl group of a starting dichloromethylvinylsilane CH_2=$CHSiCH_3Cl_2$ with the borane dimethylsulfide $BH_3 \cdot S(CH_3)_2$ as reported in the literature,[5,36,37] then the subsequent aminolysis of the resulting distilled tris(dichlorosilylethyl)borane $B(C_2H_4SiCH_3Cl_2)_3$ (C_2H_4 = $CHCH_3$, CH_2CH_2) with methylamine in THF according to our previously reported paper.[8] NCH_3 groups units were bonded to the silicon atoms to control the polymerization progress of the boron-modified polysilazane. This polymer is extremely versatile since it can be used to prepare SiBCN fibers[8] as a consequence of its good melt-spinnability and it can be used to impregnate porous materials according to its excellent solubility in common solvent such as THF or toluene. In addition, the presence of NCH_3 structural units results in a hydrophobic nature of the polymers and offers an easy access for the polymer cross-linking in an ammonia atmosphere.

3.2. Nanocasting and Thermolysis Processes. The mesoporous CMK-3 carbon was selected as a hard template. It was prepared using mesoporous SBA-15 silica as a template and sucrose as a carbon source as reported in the experimental part. It should be mentioned that the use of the carbon template prevents the interfacial contamination by diffused oxygen from the template during the thermolysis of the material confined into the nanopores of the template which, in contrast, can occur when the silica template is used. Furthermore, it should be mentioned that the use of a silica template could involve the removal of silicon nitrides along with the silica matrix during HF etching. Therefore, compared to silica template, carbon template has three main advantages: (1) chemical inertness the material confined into the nanochannels of the template at high temperature; (2) thermal stability without marked structural shrinkages; (3) hydrophobic nature that facilitated the filling of the guest polymer into the mesoporous space.

For the nanocasting process, the mass ratio between the SiBCN polymer and the CMK-3 template was fixed at 2:1 and two liquid-phase impregnations were made. It should be mentioned that the polymer confined into the channels of the CMK-3 template was cross-linked by heating to 200 °C using ammonia as cross-linking agent after each impregnation. Transamination reactions were supposed to occur during cross-linking.[8a] They allow for cross-linking and avoid loss of low-molecular-weight species from the polymer confined into the nanopores of the CMK-3 carbon. After the second cross-linking step, the as-received composite was introduced into a tubular furnace to be subjected to a thermolysis at 1000 °C in a nitrogen atmosphere (1 °C min^{-1}, dwell time of 2 h) yielding black powders in 48.7% ceramic yield (see the Supporting Information, Figure S1). To generate mesoporous SiBCN ceramics free of carbon template, our strategy was to favor the use of ammonia as carboreduction agent rather than air and thus, to avoid a possible contamination of the SiBCN material with oxygen. We used ammonia through a thermal treatment to 1000 °C. In particular, it was observed that a dweeling time of 5 h was required at 1000 °C to completely remove the carbon template resulting in weight loss of 48.9% for the composite (see the Supporting Information, Figure S2). It should be mentioned that the thermal treatment of the SiBCN ceramic in an ammonia atmosphere involved a very small weight loss (1.2%) most probably due to the removal of some free carbon in the SiBCN phase (see the Supporting Information, Figure S3).

3.3. Characterization of Mesoporous Materials. The low-angle (LA) XRD patterns of mesoporous SBA-15 silica and CMK-3 carbon templates are shown in Figure 2a and those for the SiBCN-carbon composite and the final mesoporous material free of C are shown in Figure 2b. Table 1 reports XRD parameters that have been calculated from the patterns.

The LA-XRD pattern of SBA-15 template showed three distinct diffraction peaks, which can be indexed to the (100), (110), and (200) reflections of the 2-D hexagonal space group

(39) Weinmann, M.; Kamphowe, T. W.; Fisher, P.; Aldinger, F. *J. Organomet. Chem.* **1999**, *592*, 115.

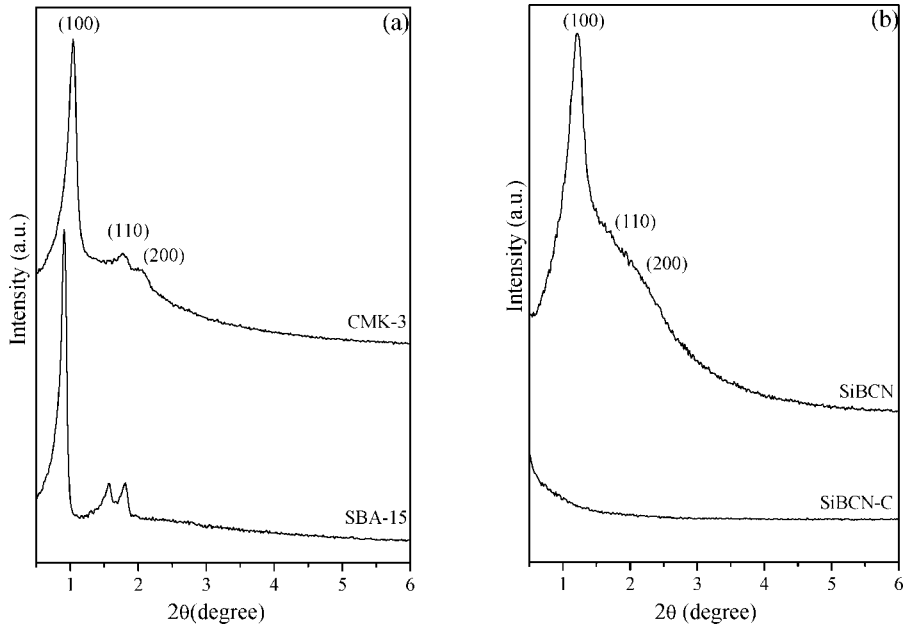

Figure 2. Low-angle XRD patterns of the (a) mesoporous silica SBA-15 and the mesoporous carbon CMK-3 templates and (b) the SiBCN-carbon composite and the mesoporous SiBCN material.

Table 1. Textual properties of Mesoporous Silica and Carbon Templates, SiBCN-C Composites, and Mesoporous SiBCN Material

	LA-XRD params		BET params		
samples	d_{100} spacing (nm)	cell param[a] α (nm)	BET surface area[b] ($m^2\ g^{-1}$)	pore diameter[c] (nm)	pore volume[d] ($cm^3\ g^{-1}$)
SBA-15	9.63	11.12	851	7.9	1.03
CMK-3	8.41	9.71	1035	3.2	0.95
SiBCN-C			123		0.14
SiBCN	7.13	8.23	600	3.6	0.61

[a] Cell parameter: $\alpha = 2d_{100}/3^{1/2}$ in the 2D hexagonal space group. [b] Specific surface areas are according to Brunauer−Emmett−Teller (BET). [c] Pore size distribution is derived from the adsorption branches of the isotherms using Barrett−Joyner−Halenda (BJH) method. [d] Total pore volumes are estimated from the amount absorbed at a relative pressure of $P/P_0 = 0.99$.

p6mm. Three similar well-resolved diffraction peaks could be identified in the XRD pattern of the CMK-3 template at 1.04, 1.78, and 2.01°, respectively. In contrast, there are no diffraction peaks in the corresponding XRD pattern for the as-obtained SiBCN−carbon composite as shown in Figure 2b suggesting the absence of mesoporosity. After removal of the carbon template, a strong diffraction peak attributed to the (100) diffraction peak of the hexagonal *p6mm* symmetry appeared in the corresponding XRD pattern (Figure 2b). The d_{100} value was calculated to be 7.13 nm (Table 1). As a consequence, the cell parameter was deduced to be 8.23 nm.

This (100) peak is asymmetric suggesting to us the presence of nondiscernible peaks and most probably, the presence of the (110) and (200) reflections. As a consequence, it can be proposed that the final SiBCN sample displays an ordered 2D hexagonal mesostructure as a negative replica of the carbon CMK-3. By scanning from 10 to 80°, the mesoporous material appeared X-ray amorphous as described in our preceding paper[8] and generally observed for SiBCN materials prepared from boron-modified polysilazanes.[5,10] To gain further information on the overall structure of the mesoporous material, we investigated Raman and FT-IR spectroscopies. Furthermore, comparison was made with the bulk material, which also appeared X-ray amorphous, obtained from the same polymer and under identical cross-linking and thermolysis conditions. Unfortunately, Raman spectroscopy did not offer fundamental insight on the structural arrangement of the samples prepared at 1000 °C. Indeed, no peak was detected for the mesoporous material, whereas the Raman spectrum of the bulk material showed two poorly discernible peaks, which are the typical features of disordered graphitelike carbon, namely the *D* peak located at around 1350 cm^{-1}, and the *G* peak centered around 1590 cm^{-1}.[40] Such diffuse peaks are in general found for SiCN materials containing free carbon phase produced at 1000 °C.[41] This points to the fact that the quantity of free carbon in the mesoporous material can be considered lower than that in the bulk material.

Infrared spectroscopy gave more information concerning the structural arrangement of the SiBCN material. Figure 3 shows the IR spectra of the mesoporous SiBCN and the bulk SiBCN materials. Both spectra are similar.

A main absorption peak at around 880−890 cm^{-1} is attributed to the stretching vibration of Si−N−Si bonding.[42] Another main absorption peak around 1390 cm^{-1} is assigned to the in-plane stretching of sp^2 B−N bond.[43] The shoulder corresponding to N−H bonding at about 3300 cm^{-1} is also present[44] indicating the presence of residual hydrogen within the final material. This is probably due to the low final

(40) Zerda, T. W.; Tu, W.; Zerda, A.; Zhao, Y.; Von Dreele, R. B. *Carbon* **2000**, *38*, 355.
(41) Kleebe, H.-J.; Störmer, H.; Trassl, S.; Ziegler, G. *Appl. Organomet. Chem.* **2001**, *15*, 858.
(42) Smirnova, T. P.; Badalian, A. M.; Yakovkina, L. V.; Kaichev, V. V.; Bukhtiyarov, V. I.; Shmakov, A. N.; Asanov, I. P.; Rachlin, V. I.; Fomina, A. N. *Thin Solid Films* **2003**, *429*, 144.
(43) Duperrier, S.; Gervais, C.; Bernard, S.; Cornu, D.; Babonneau, F.; Miele, P. *J. Mater. Chem.* **2006**, *16*, 3126.
(44) Mar, K. M.; Sammuelson, G. M. *Solid State Technol.* **1980**, *23*, 137.

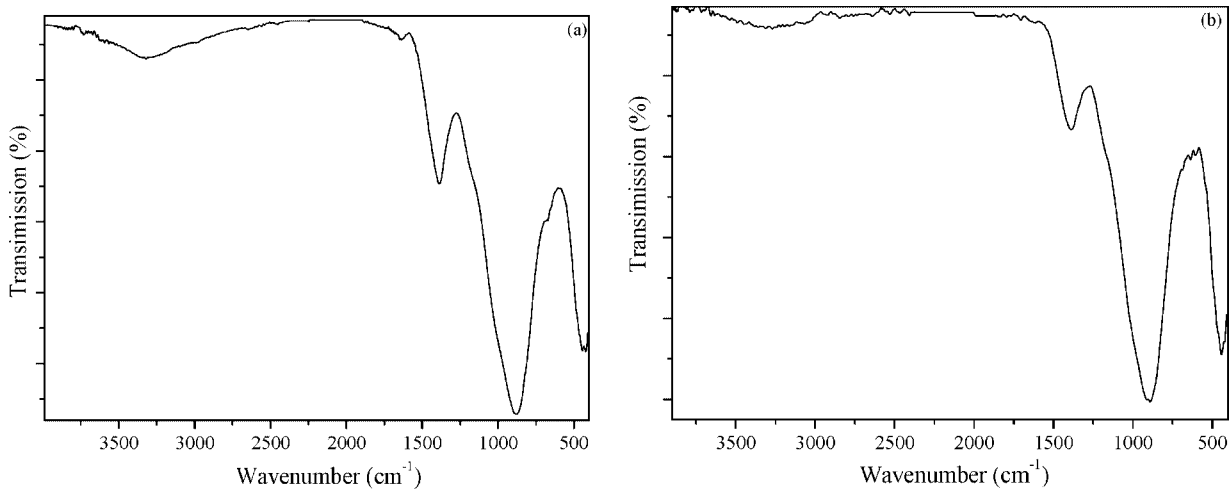

Figure 3. FTIR spectra of the (a) mesoporous and (b) bulk material derived from the boron-modified polysilazane of the type $B(C_2H_4SiCH_3NCH_3)_3]_n$ (C_2H_4 = $CHCH_3$, CH_2CH_2).

temperature of the thermolysis which was applied, i.e., 1000 °C, to prepare the samples.

Ordered structural regularity of the mesoporous SiBCN material was investigated using TEM. Figure 4 shows the TEM images of the SBA-15 and CMK-3 templates and the mesoporous SiBCN material.

For the host matrix SBA-15 (images a and b in Figure 4), TEM images confirmed the 2D hexagonal mesoporous structure with a high structural regularity in large domains. Similarly, the hexagonal symmetry of CMK-3 as the negative replication of the SBA-15 could be also confirmed by the observation of TEM (images c and d in Figure 4). TEM images of the template-free SiBCN sample (images e and f in Figure 4) revealed that the structure of the final product consists of a highly ordered hexagonal arrangement of cylindrical channels, which is similar to the structure of original mesoporous SBA-15 silica. As a consequence, it can be concluded that the geometry of the original silica template is retained in the final SiBCN product through the double casting pathway. The distance between the centers of the adjacent channels is approximately 8 nm, which is in agreement with the cell parameter (8.23 nm; Table 1) calculated from the d_{100} value found in the XRD pattern. Therefore, it can be confirmed that the SiBCN material displays typical 2-D hexagonal *p6mm* symmetry.

The morphology of the mesoporous SBA-15, CMK-3, and SiBCN was also studied using SEM. Figure 5 displays the SEM images of the original mesoporous silica host, as well as carbon template and SiBCN product.

The morphology of the mesoporous SiBCN material is similar to that of the silica and carbon templates. Each material exhibited monodispersed particles with a uniform size of about 1 μm. This similarity in the surface morphology of all samples confirmed that the surface morphology of the mesoporous silica and carbon hosts is retained in the SiBCN samples. This also confirmed the fact that the polymer displays an excellent ability to fill the nanopores of the carbon template and to be retained inside the nanopores of the template without depolymerization. To provide information about chemical composition, the mesoporous material produced at 1000 °C was analyzed by elemental analysis and XPS. It should be mentioned that samples were heated under a vacuum to 200 °C overnight before performing elemental analyses under inert conditions. Mesoporous SiBCN materials of an empirical formula $Si_{3.0}B_{1.0}C_{4.2}N_{3.5}$ (Si, 42.3 wt %; B, 5.5 wt %; C, 25.2 wt %; N, 25.1 wt %) have been produced using curing to 200 °C in an ammonia atmosphere, thermolysis to 1000 °C in a nitrogen atmosphere, and then ammonia thermal treatment to 1000 °C. For comparison, bulk SiBCN materials were analyzed. They were produced from the same polymer using identical thermal conditions except for the last step using ammonia which was omitted. An empirical formula of $Si_{3.0}B_{1.0}C_{4.7}N_{2.5}$ was found. It corresponds to the following composition: Si, 45.2 wt %; B, 5.8 wt %; C, 30.1 wt %; N, 18.7 wt %. It should be mentioned that oxygen values were found to be lower than 2 wt % for both samples and were therefore omitted in the calcul of empirical formulas. According to these results, it is clear for the mesoporous material that the carbon template was completely removed after the thermal treatment to 1000 °C in an ammonia atmosphere. In addition, the mesoporous material released after post-thermolysis treatment under ammonia ($Si_{3.0}B_{1.0}C_{4.2}N_{3.5}$) retained a lower amount of carbon and a higher amount of nitrogen compared with those obtained for the as-made bulk material ($Si_{3.0}B_{1.0}C_{4.7}N_{2.5}$). This result points to the fact that there is either nitrogen incorporation in the mesoporous material or carbothermal reaction with free carbon initially present in the SiBCN material. However, it should be mentioned according to the empirical formula of the mesoporous material that the latter contains free carbon.

Moreover, the Si:B ratio fixed in the boron-modified polysilazane ($[C_{14.4}H_{31.4}N_{4.1}B_{1.0}Si_{3.0}]_n$) is maintained as well in the derived mesoporous as in the bulk materials. In both cases and in particular for the mesoporous material, these observations corroborate definetely the fact that volatilization of low-molecular-weight species (evaporation of polymer fragments) due to chain scission and back-biting, which could be considered with such "low-molecular-weight" polymers is avoided during the thermolysis in a nitrogen atmosphere.

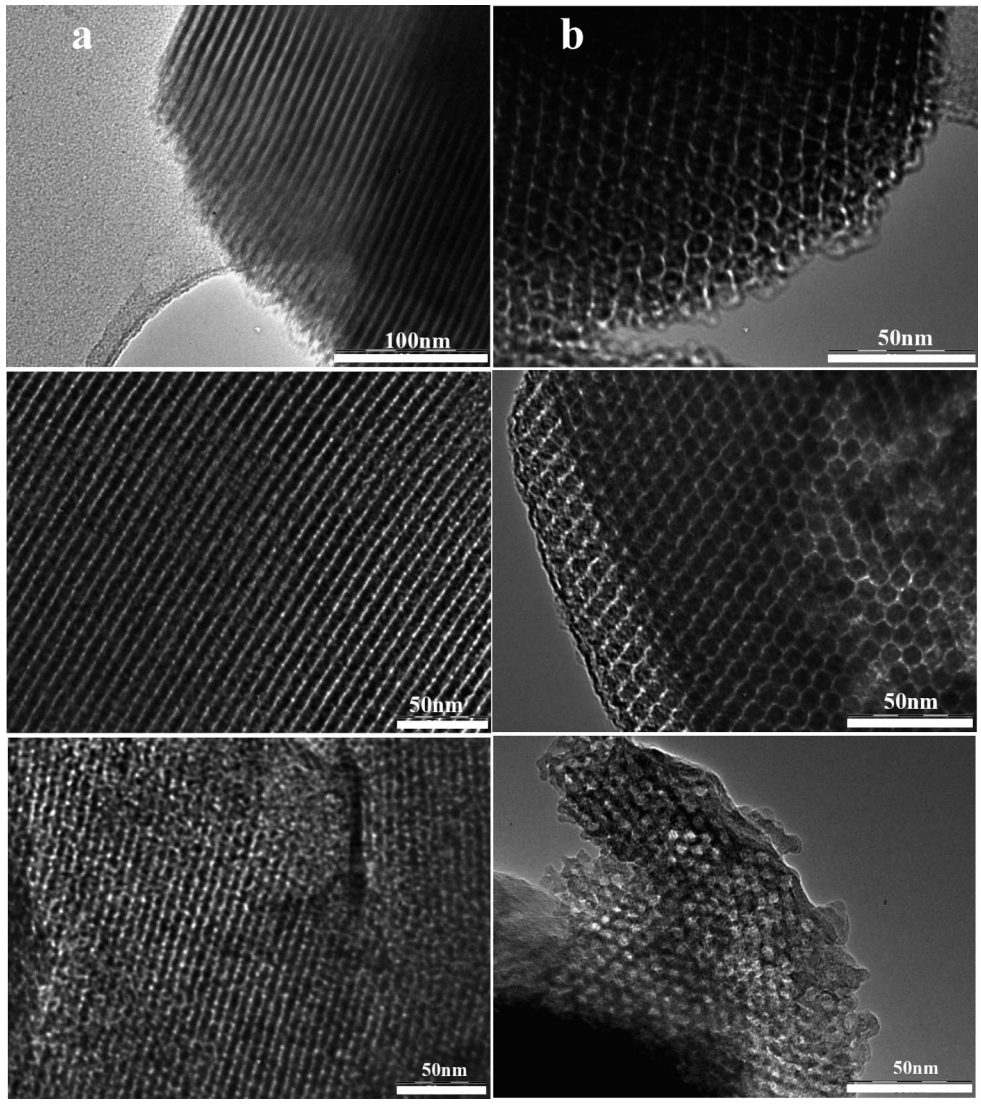

Figure 4. TEM images of (a, b) the mesoporous silica SBA-15, (c, d) the mesoporous carbon CMK-3 and (e, f) the mesoporous SiBCN taken along the [110] and [100] directions, respectively.

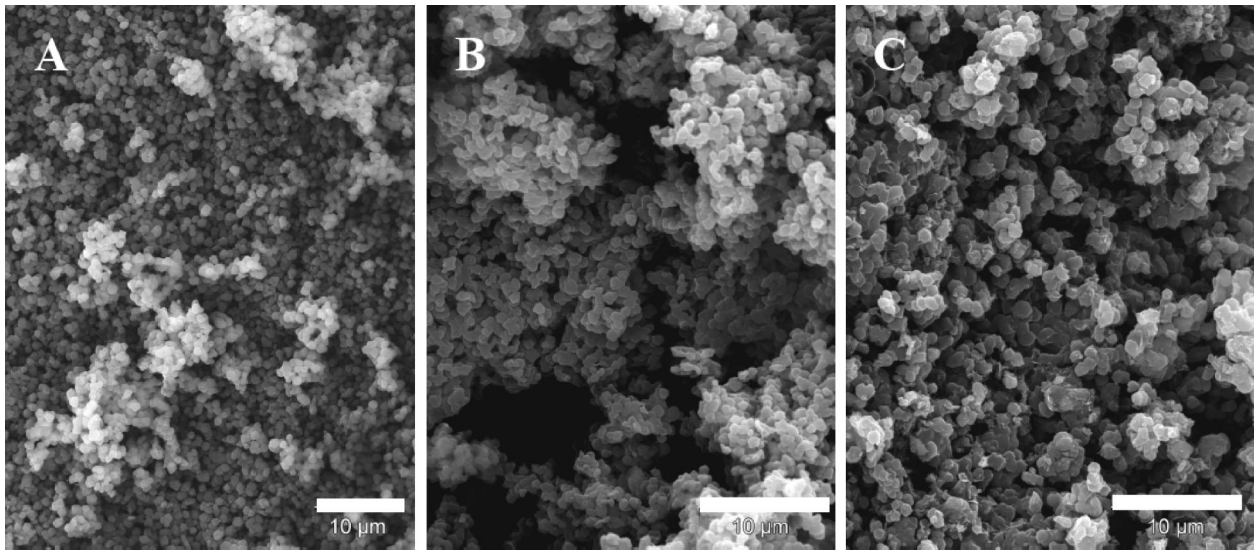

Figure 5. SEM images of the (a) mesoporous silica SBA-15 template, (b) the mesoporous carbon CMK-3 template, and (c) the mesoporous SiBCN material. The scales are all 10 μm.

The chemical environment around the Si, B, C, and N atoms in the mesoporous materials was investigated by XPS spectroscopy. Figure 6 displays the characteristic peaks attributed to Si, B, C, and N environments.

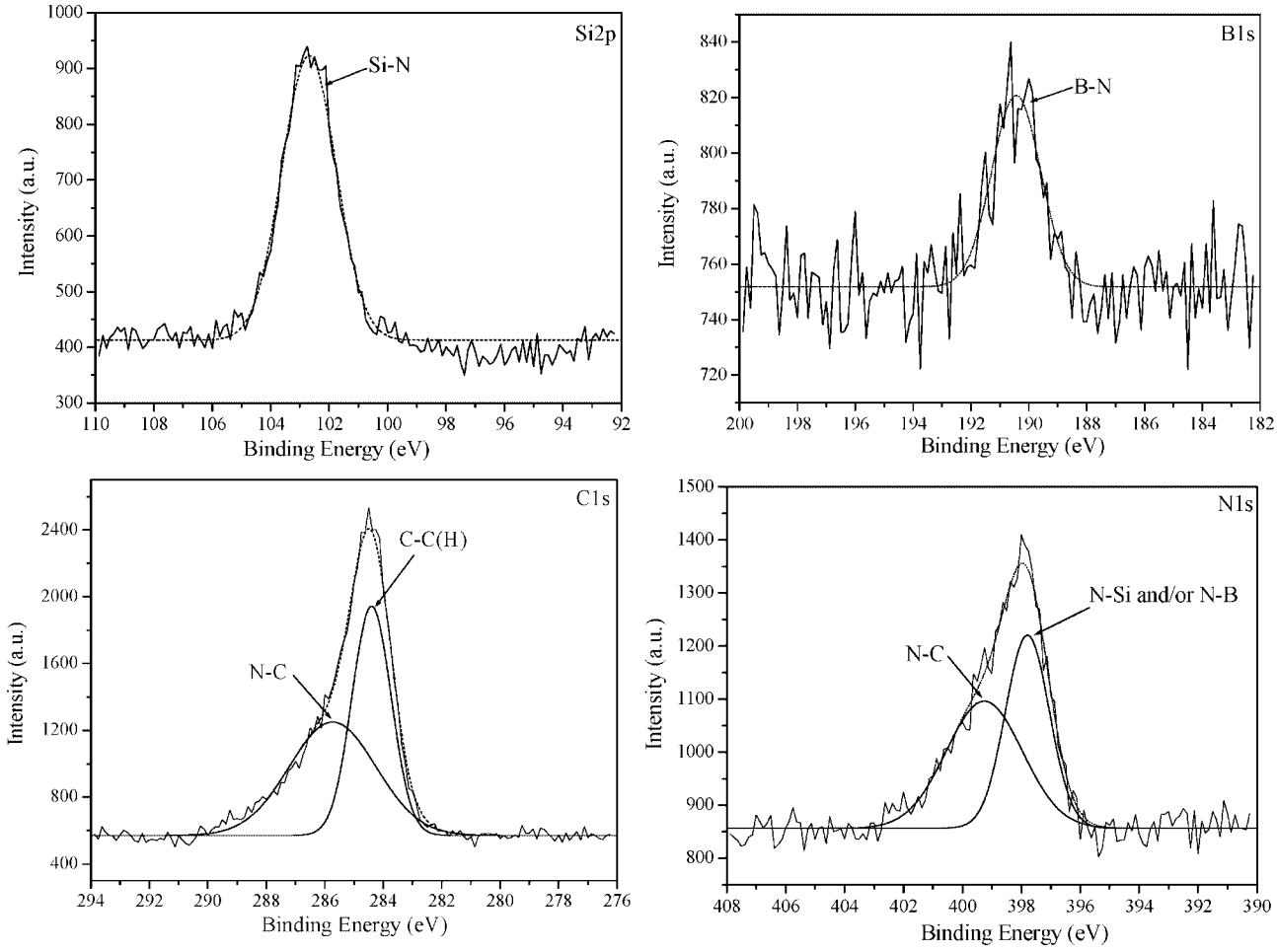

Figure 6. High-resolution Si (2p), B (1s), C (1s), and N (1s) XPS spectra of the mesoporous SiBCN material.

The Si2p peak centered at 102.9 eV is exclusively attributable to Si−N bonding,[45] which was identified in the corresponding FT-IR spectrum (Figure 3) and the B1s peak at 190.3 eV corresponds to the B−N bonding which was found in the corresponding FT-IR spectrum.[46] The C1s peak can be split into two simulated peaks at 285.7 and 284.4 eV, which corresponds to the C−N bonding and C−C (or C−H) bonding, respectively.[45] The N1s peaks clearly can be split into two simulated peaks, in which the first at 399.3 eV is characteristic of the N−C bonding, whereas the second at 397.8 eV is attributed to N−Si and/or N−B bonding.[45–47] However, it should be pointed out that there is no detectable C(1s) Si signal at 282.8 eV, which is also confirmed by the absence of Si(2p) C signal around 100.3 eV, indicating negligible Si−C bonds in the mesoporous SiBCN in good agreement with FT-IR spectroscopy.

Figure 7 shows the N_2 adsorption−desorption isotherms and the corresponding pore-size distribution curves of the mesoporous SBA-15, CMK-3, and SiBCN materials. Table 1 reports BET parameters.

Both isotherms of silica and carbon templates are of type IV with a hysteresis loop at a relative pressure of approximately 0.67 and 0.45, respectively. In addition, as shown in Table 1, the specific surface area was measured to be 851 $m^2\ g^{-1}$, while the pore diameter was found to be 7.9 nm for the silica template. For the carbon template, the specific surface area was measured to be 1035 $m^2\ g^{-1}$ and the pore diameter was found to be 3.2 nm. Concerning the SiBCN-C composite, it is interesting to note that there is no hysteresis loop in the nitrogen isotherm in the pressure range of capillary condensation in primary mesopores of the template (isotherm of type I). The specific surface area decreased to 123 $m^2\ g^{-1}$ and the pore volume could not be measured. Such results are consitent with LA-XRD data (Figure 2b) and tend to indicate that the nanochannels have been fully filled by the polymer during the nanocasting pathway and that the material is retained into the nanochannels of the CMK-3 template during the polymer-to-ceramic conversion. In contrast, after removal of the carbon template, the nitrogen isotherm of the as-received SiBCN sample showed a clear step at a relative pressure of about 0.5, which is attributed to capillary condensation in ordered mesoporous structures. The corresponding specific surface area is calculated to be 600 $m^2\ g^{-1}$ and the deduced pore volume is 0.61 $cm^3\ g^{-1}$ (Table 1). Moreover, the narrow pore-distribution centered at 3.6 nm appears more spread than that of the

(45) Moulder, J. F.; Stickle, W. F.; Sobol, P. E.; Bomben, K. D. *Handbook of X-ray Photoelectron Spectroscopy*; Perkin-Elmer: Eden Prairie, MN, 1992.
(46) Kim, S. Y.; Park, J.; Choi, H. C.; Ahn, J. P.; Hou, J. Q.; Kang, H. S. *J. Am. Chem. Soc.* **2007**, *129*, 1705.
(47) Tarntair, F. G.; Wen, C. Y.; Chen, L. C.; Wu, J. J.; Chen, K. H.; Kuo, P. F.; Chang, S. W.; Chen, Y. F.; Hong, W. K.; Cheng, H. C. *Appl. Phys. Lett.* **2000**, *76*, 2630.

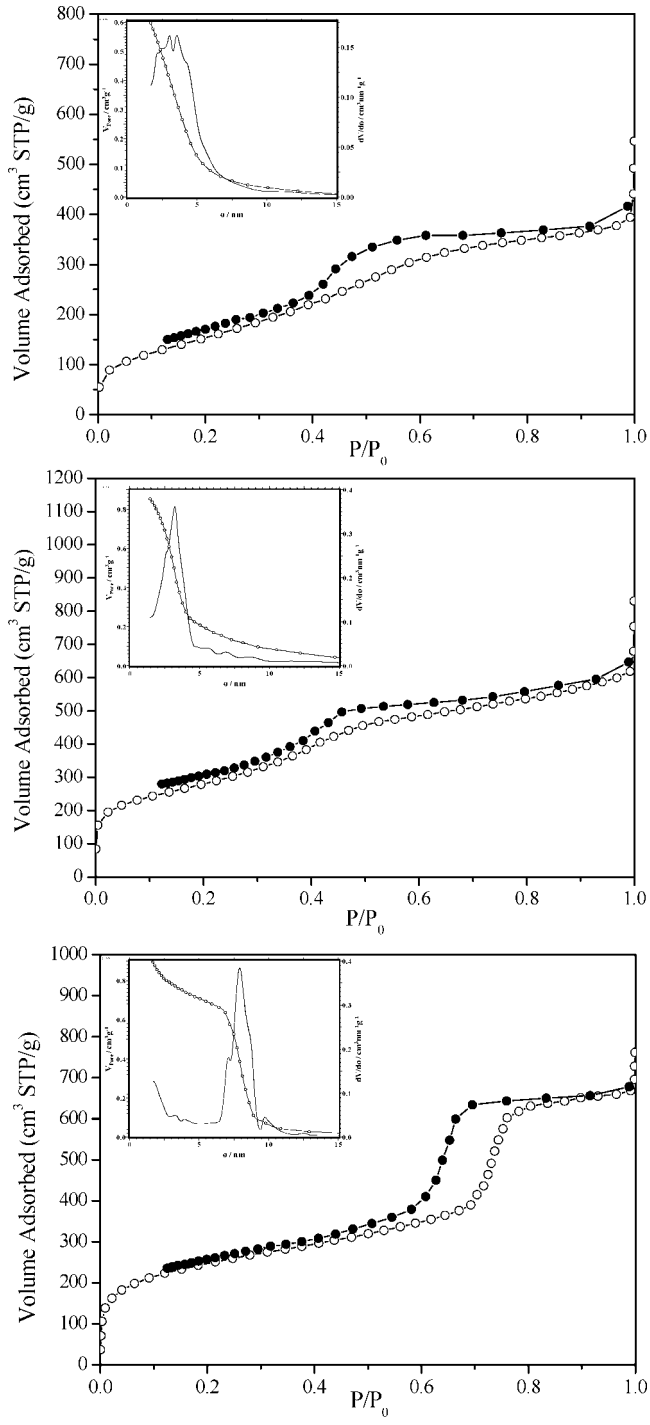

Figure 7. Nitrogen adsorption−desorption (○ and •, respectively) isotherms of (a) the mesoporous SBA-15 template, (b) the mesoporous CMK-3 template, (c) and the mesoporous SiBCN material. The pore size distribution curves are shown inset.

carbon template. In addition, the corresponding cell parameter is lower than that of the CMK-3 and SBA-15, which is due to framework shrinkage that occurred during the polymer-to-ceramic conversion.

The oxidation behavior at high temperature of the mesoporous $Si_{3.0}B_{1.0}C_{4.2}N_{3.5}$ material derived from ($[C_{14.4}H_{31.4}N_{4.1}B_{1.0}Si_{3.0}]_n$) was studied under air by means of HT-TGA from 25 to 1400 °C (10 °C min^{-1}) (Figure 8).

The mesoporous material showed an excellent stability in air with a small detectable weight change when heating to

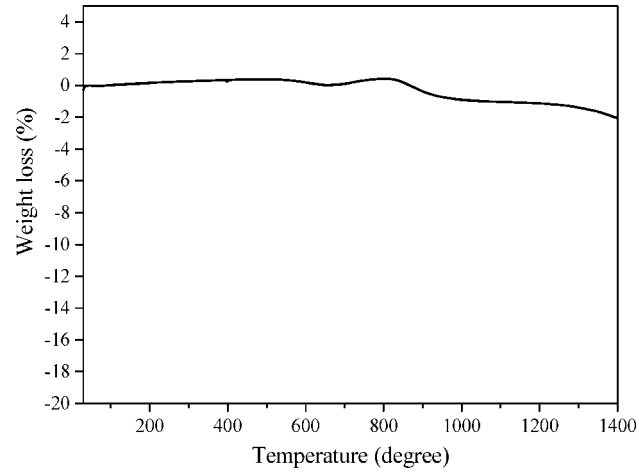

Figure 8. Oxidation behavior of the mesoporous $Si_{3.0}B_{1.0}C_{4.2}N_{3.5}$ material in the temperature range RT, 1400 °C (heating rate, 10 °C/min; flowing air).

1400 °C. Particularly, the TGA curve can be shared into three temperature ranges. A first range could be considered from RT to 660 °C in which almost no weight changes were measured. A second range from 660 to 810 °C corresponded to a small weight increase (+0.41 wt % measured at 810 °C). In a three range from 810 to 1400 °C, oxidation in air proceeded with a continuous weight loss from +0.41 wt % to −2.05 wt %.

In comparison, it should be mentioned that there was only a slight weight increase (+2.9 wt %) detectable during the oxidation treatment from 1100 to 1500 °C for the SiBCN fibers that had been described in our previous paper using the same polymer.[8] We attributed this weight gain to the formation of silica from the silicon carbide and silicon nitride phases which were identified in the fibers according to eqs 1 and 2.

$$2SiC(s) + 3O_2(g) \rightarrow 2SiO_2(s) + 2CO(g) \quad (1)$$

$$Si_3N_4(s) + 3O_2(g) \rightarrow 3SiO_2(s) + 2N_2(g) \quad (2)$$

It should be mentioned that silicon nitride was identified in the mesoporous material studied in the present paper through the presence of Si−N bonds in the FT-IR spectrum (Figure 3) and the XPS spectrum (Figure 6). In addition, boron nitride was identified in FT-IR and XPS spectra (Figures 3 and 6). It is known that boron nitride is oxidized to boric oxide when exposed to oxygen and moisture at intermediate temperatures (800−900 °C) according to eqs 3 and 4.[48]

$$4BN(s) + 3O_2(g) \rightarrow 2B_2O_3(l) + 2N_2(g) \quad (3)$$

$$2BN(s) + 3H_2O(g) \rightarrow B_2O_3(l) + 3H_2(g) + N_2(g) \quad (4)$$

In addition, it is known that boric oxide is most likely released as vapor from the sample at higher temperature range (1200 °C) with ambient water vapor to form the volatile species HBO_2 according to eq 5[48,49]

$$B_2O_3(l) + H_2O(g) \rightarrow 2HBO_2(g) \quad (5)$$

Oxidation of boron nitride is sensitive to crystalline quality and porosity. For example, a decrease of the crystallinity of the boron nitride phase causes a decrease of the temperature of oxidation.[48]

The two oxidation products in eqs 1–5, i.e., silica and boric oxide, are supposed to be in interaction during the oxidation process of SiBCN materials and form a borosilicate glass exhibiting a lower decomposition temperature than silica.

Lastly, it should be mentioned that free carbon is expected to be oxidized to carbon monoxide.

On the basis of these remarks, complex mechanisms occur during the oxidation process of mesoporous SiBCN materials with either weight increases (eqs 1–4) or weight losses (eq 5 and oxidation of carbon). According to the lower oxidation temperature of boron nitride compared with silicon nitride and silicon carbide, it is reasonable to suggest that the slight weight increase of 0.41 wt % at intermediate temperatures (660−810 °C) is mainly induced by oxidation of the poorly crystallized boron nitride phase resulting in the formation of boric oxide according to eqs 3 and 4. The formation of boric oxide at intermediate temperatures contributes to enhance silicon nitride and silicon carbide oxidation to silica above 810 °C. The second part of the oxidation process from 810 to 1400 °C is extremely complex and there is a lack of evidence or discussion in the literature to support our contentment with regards to the oxidation mechanisms of mesoporous SiBCN materials which occur in this temperature range. We speculate that the continuous weight loss from +0.41 to −2.05 wt % caused by several mechanisms including formation of silica (eq 1 and 2; weight gain, reaction of silica with boric oxide to form borosilicate glass and evaporation of boric oxide out of the glass by residual water vapor (eq 5); weight loss).

The difference in the TGA curve profil between SiBCN fibers[8] and mesoporous SiBCN materials obtained from the same polymeric system results from the difference in the specific surface area of both samples. SiBCN fibers are supposed to have low specific surface area, whereas the mesoporous powders display high specific surface area as mentioned in the present paper. In the case for fibers, we suggested that oxidative attack occurred at the surface of the fibers by formation of a passivating amorphous oxide layer upon oxidation. The latter offered protection to further oxidation by hindering diffusion-controlled oxidation.[8] In contrast, we postulate that oxidation in mesoporous materials occurred by inward diffusion of oxygen due to the presence of nanochannels resulting in a higher sensitivity of the material against oxygen. However, mesoporous SiBCN materials can be considered as catalyst supports to effectively increase the service life of devices that have to withstand harsh oxidative and thermal environments.

4. Conclusions

Novel open, continuous, ordered 2D hexagonal mesoporous SiBCN materials with high BET surface area and narrow pore-size distribution were successfully prepared using boron-modified polysilazane of the type $[B(C_2H_4SiCH_3NCH_3)_3]_n$ as preceramic polymer and mesoporous carbon CMK-3 as hard template. The mesoporous SiBCN ceramic obtained was the negative replica of its host carbon template and similar to the original silica template. It was X-ray amorphous and displayed an empirical formula of $Si_{3.0}B_{1.0}C_{4.2}N_{3.5}$. According to the high durability of the mesoporous $Si_{3.0}B_{1.0}C_{4.2}N_{3.5}$ material, the nanocasting pathway with hard templates opens the door to the design of highly porous SiBCN structures that could be applied in harsh oxidative and thermal environments.

Acknowledgment. This work was funded by the Marie Curie incoming International Fellowship European Community (MIF1-CT-2006-021864). The authors thank Dr. Gang Chen for XPS measurements and Didier Fournier for FT-IR/ATR spectroscopy. The authors acknowledge supporting co-workers at the LMI of Lyon and, in particular, Fernand Chassagneux for BET discussions. We gratefully acknowledge the CTμ (Centre Technologique des Microstructures) of the Université Lyon 1 for access to the SEM apparatus.

Supporting Information Available: TGA curves (PDF). This material is available free of charge via the Internet at http://pubs.acs.org.

CM703114Y

(48) Jacobson, N.; Farmer, S.; Moore, A.; Sayir, H. *J. Am. Ceram. Soc.* **1999**, *82*, 393.
(49) Gogotst, Y. G.; Lavrenko, V. A. *Corrosion of High-Performance Ceramics*; Springer-Verlag: Berlin, 1992.